

# Cyclone Tracking using Multiple Satellite Image Sources

Anand Panangadan  
Jet Propulsion Laboratory  
California Institute of  
Technology  
Pasadena, CA 91109  
{Anand.V.Panangadan,shen.shyang.ho,Ashit.Talukder}@jpl.nasa.gov

Shen-Shyang Ho  
Jet Propulsion Laboratory  
California Institute of  
Technology  
Pasadena, CA 91109

Ashit Talukder  
Jet Propulsion Laboratory  
California Institute of  
Technology  
Pasadena, CA 91109

## ABSTRACT

We present an automated cyclone tracking system that uses images from multiple satellite sources. The system tracks cyclones using infrared images from a Geostationary Operational Environmental Satellite (GOES), precipitation images derived from five satellite sources, and ocean surface wind field satellite images. The system consists of three main components: (i) data preprocessing steps for each data source, (ii) cyclone eye detection algorithms for each data source, and (iii) a filter-based tracker that integrates the eye detection results from each data source. Experimental results show that our prototype system is operationally feasible and has better performance than our prior cyclone tracking system.

## Categories and Subject Descriptors

I.4.7 [Image Processing and Computer Vision]: Feature Measurement—*Feature representation*; H.3.3 [Information Systems]: Information Storage and Retrieval—*Selection process*; J.2 [Physical Sciences and Engineering]: [Earth and atmospheric sciences]

## General Terms

Algorithms, Design

## Keywords

Object Tracking, Hough Transform, Particle Filter

## 1. INTRODUCTION

Tropical cyclones are low-pressure weather systems that develop over the warm tropical water of the oceans with “organized deep convection and a closed surface wind circulation about a well-defined center”<sup>1</sup>. In the United States, the National Oceanic and Atmospheric Administration’s National Hurricane Center (NOAA-NHC) is responsible for

<sup>1</sup><http://www.nhc.noaa.gov/aboutgloss.shtml>.

©2009 Association for Computing Machinery. ACM acknowledges that this contribution was authored or co-authored by a contractor or affiliate of the [U.S.] Government. As such, the Government retains a nonexclusive, royalty-free right to publish or reproduce this article, or to allow others to do so, for Government purposes only.  
ACM GIS '09, November 4-6, 2009, Seattle, WA, USA  
©2009 ACM ISBN 978-1-60558-649-6/09/11...\$10.00

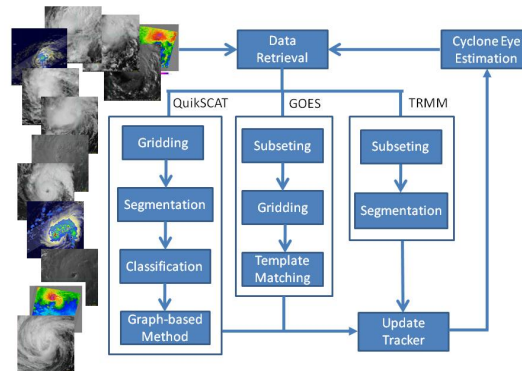


Figure 1: System Overview for the Automated Cyclone Tracking System.

tracking tropical cyclones and issuing forecasting bulletins, warnings, and advisories about tropical cyclones. The tracking task is *manually* performed using data from satellites, radar, reconnaissance aircraft, and ships, and surface observations from land stations and data buoys.

Manual shape-matching techniques have been extensively used to estimate a cyclone’s intensity and to predict its future intensity based on cloud features in infrared images [2]. The cyclone eye locations have also been determined from QuikSCAT wind field images “subjectively by observation” [3] with a mean distance error of 33.3 km and 21.2 km between the detected eye location and the NHC best-track estimate for images with 25 km and 2.5 km spatial resolution, respectively. Zhang et al. [7] proposed a variant of contour tracking for cyclone eye tracking which was demonstrated on a sequence of only 16 satellite infrared images. A Kalman filter-based approach for cyclone tracking using wind field satellite data and precipitation data was recently proposed [4]. The approach, however, does not have the capability to accurately detect the cyclone eye. Moreover, the low temporal resolution of the satellite measurements makes accurate tracking of the cyclone eye challenging.

We describe an automated cyclone tracking system that can track cyclones using only data from multiple satellite sources (no *in situ* measurements). The main contribution of our paper is a system (see Figure 1) that improves on

the methodology proposed in [4] and augments the current *manual* tropical cyclone tracking operation. In addition, a variant of the Hough-transform voting scheme for cyclone eye detection in wind field images is introduced in this paper.

## 2. IMAGE SOURCES

Here, we describe the data sources used in our system.

**Infrared images:** We use images from the Imager instrument carried aboard the GOES-12 satellite. The GOES-12 satellite is located over 75 W longitude and can observe the continental United States and the Atlantic ocean. The infrared images captured at wavelengths of approximately 11  $\mu\text{m}$  (Channel 4) are most useful for tracking storm clouds. The images are available every 30 minutes.

**TRMM-adjusted Merged Precipitation Image:** We use the merged precipitation data called the 3B42 data. The 3B42 data quantifies global rainfall every 3 hours with each pixel representing a square region of dimension  $0.25^\circ$  with values ranging from  $0\text{mm}/h$  to  $100\text{mm}/h$ .

**Wind Field Images:** The QuikSCAT satellite carries a specialized microwave radar that measures near ocean surface wind speed and direction under all weather and cloud conditions [1]. The satellite orbits the Earth with a 1800 km wide measurement swath. The scatterometer is able to provide measurements over a particular region twice per day. We utilize the Level 2B data which consists of rows of ocean wind vectors in 25km and 12.5km wind vector cells.

## 3. SYSTEM DESIGN

A system that integrates information from multiple data sources has to be designed in such a way to exploit the disparate characteristics of the different data sources while ensuring that deficiencies in any one data source do not adversely affect the functioning of the entire system. Polar orbiting satellites do not monitor a region continuously and have a revisit rate of approximately 12 hours (low temporal frame rate). However, the relatively low orbit enables them to carry remote-sensing instruments that can measure useful surface parameters such as ocean surface wind velocities (QuikSCAT data). On the other hand, geostationary satellites observe the same portion of the earth's surface continuously and thus can provide data with a high temporal rate. The GOES infrared images, together with the QuikSCAT images and the TRMM-adjusted precipitation images, improves the temporal resolution for cyclone tracking from an upper bound time interval of one image every three hours [4] to every half-hour.

In addition, the different instruments have varying spatial resolutions and coverage characteristics. In our system, we have independent data preprocessing steps for each distinct data source (Figure 1). We then apply different eye detection algorithms that are appropriate to each data source to locate the hurricane center. Only the results from each of these eye location algorithms are integrated using a filter-based tracker. This predictive tracker enables the system to output cyclone location estimates even when satellite data is not immediately available. The filter provides two benefits to our cyclone tracking system. Firstly, the tracker provides cyclone location estimates as new satellite data becomes available. This information is then used to constrain the search region for the cyclone eye detection algorithms. This reduction in the search region reduces the incidence

of false positives and reduces the computational processing time. Secondly, the filter state estimates are smoothed versions of the sequence of observations (cyclone eye identified by the eye detection algorithms). These estimates reduce the affect of random errors in the observations.

## 4. SYSTEM COMPONENTS

In this section, we describe in detail the main components in our cyclone tracking system shown in Figure 1.

### 4.1 Data Preprocessing

Data preprocessing is done differently for different satellite data. The GOES images are subseted based on the search region estimate from the tracker. Then, nearest neighbor interpolation is used for image gridding on the subseted region. Since wind vector field provides good indicator for cyclone, the QuikSCAT image swath is gridded for global cyclone detection without any subsetting. For the TRMM-adjusted merged precipitation data, no gridding is necessary since it is gridded data. One needs only to subset the region based on the search region estimate from the tracker.

### 4.2 Cyclone Eye Detection

Since the satellite image features from the three satellite sources are fundamentally different, feature-based cyclone eye detection algorithms have to be designed independently for images from different satellite sources.

#### 4.2.1 QuikSCAT: Graph-based Method

For the QuikSCAT images, cyclone eye detection consists of 3 main steps:

1. *Segmentation* using the wind speed value at each pixel for identifying the Region of Interest (ROI) in the QuikSCAT image [5].
2. *Ensemble classification* using wind speed histogram, wind direction histogram, speed-to-direction histograms, dominant wind direction (DOWD) measure, and relative wind vorticity to decide whether a ROI contains a cyclone [4].
3. Graph-based (GB) cyclone eye detection algorithm (see Algorithm 1) works as follows.
  - (a) An arc (directed edge) is computed for each pixel based on the normal vector of the wind direction at each pixel.
  - (b) The arc points to one of the eight neighbors for each pixel.
  - (c) The likely eye locations are those that have many neighbors pointing at them. These pixels are in the  $VC$  set.
  - (d) A recursive depth-first search algorithm is used for computing the spanning tree sizes for the pixels in  $VC$  as the root nodes.
  - (e) The root node that grows the largest spanning tree is the cyclone eye.

```

Input: QuikSCAT L2B Image with  $m$  pixels.
Output:  $S$ , Cyclone Eye
foreach  $P_{i \in \text{Pixel}}$  do
  Compute the normal vector  $\hat{n}_i$  to the direction
  vector  $\hat{d}_i$ ;
  Calculate which 8-neighbors  $\hat{n}_i$  is pointing;
  Update the neighbor count  $N_k$  of the pixel  $k$   $\hat{n}_i$  is
  pointing;
  Update  $l_k$ , list of neighbor pixels, pointing at  $k$ 
end
 $MaxNeighbor = \max_{1 \leq k \leq m} N_k$ .
 $VC = \{i \mid N_i \geq MaxNeighbor - 1\}$ ;
foreach  $j \in VC$  do
   $root \leftarrow j$ ;
   $Count[j] = SizeOfSpanningTree(root, l_{root})$ 
end
 $S = \arg \max_{j \in VC} Count[j]$ ;

```

**Algorithm 1:** Graph-based (GB) cyclone eye detection.

#### 4.2.2 GOES: Template Matching

A hurricane is a cyclone of high wind intensity. As a hurricane increases in wind intensity, its cloud patterns begin to resemble a log-spiral with an approximately  $10^\circ$  pitch and centered at the hurricane eye [2]. This characteristic pattern has been used to locate the hurricane eye using both manual and automatic matching of log spiral-shaped templates. We base our GOES eye detection method on the Spiral Centering routine used by Wimmers and Welden [6].

#### 4.2.3 TRMM: Object Centroid

For a TRMM image, segmentation using the precipitation rate at each pixel is performed to detect the cyclone in the search region estimated by the tracker. The centroid of the segmented region is estimated to be the eye, as in [4].

### 4.3 Cyclone Tracking

The cyclone eye detection algorithms work best when the image to be searched covers predominantly the hurricane region as the presence of other features could lead to false positives. Thus, it is necessary to confine the search space for the eye detection algorithms while still ensuring that the image contains the cyclone to be detected. In addition, restricting the size of the images to be searched decreases the time required to run the computationally intensive eye detection algorithms. In our system, we use a state and observation model-based tracker to predict the likely cyclone location in the satellite images. The eye detection algorithms (for TRMM and GOES images) then consider only the area around this predicted location.

We use a Kalman filter or a particle filter as the tracking mechanism. In our application, the state of the filter corresponds to the estimate of the cyclone location and its velocity. The observations correspond to the detected cyclone eyes by the individual eye detection algorithms. We used a simple state evolution model - only the velocity is used to predict the future location. The observation model specifies the probability of the eye detection algorithms returning a location given the true eye location. We have assumed that both the state and observation models have additive zero-mean Gaussian noise, the variances of which are parameters of the tracking algorithm.

## 5. EXPERIMENTAL RESULTS

We use the *detected eye error* as the performance metric for system evaluation. This is defined as the distance between the cyclone eye location as detected by our algorithms and output by the tracker and the cyclone eye estimate provided by the NHC (“best track”). The NHC best-track is available only at fixed 6-hour intervals. Hence we interpolate (linear interpolation) the best track to obtain the NHC estimate at the same instant when a satellite data image becomes available.

### 5.1 QuikSCAT GB Algorithm

We compare the performance of the GB algorithm with the object centroid method (Centroid) [4]. Table 1 shows the performance comparison on 12.5 km spatial resolution L2B QuikSCAT image sequences for two major hurricanes in the North Atlantic Ocean. GB-II denotes Algorithm 1 where the VC set includes pixels with at least  $MaxNeighbor - 1$  neighbors pointing towards them. GB-I is a variant where the VC set consists of pixels with  $MaxNeighbor$  neighbors pointing towards them. GB-II uses a larger search space than GB-I and hence its performance is much better than GB-I. Note that the larger search space lowers the detected eye error with a slight increase in computational cost. GB-II is used in our system.

Hurricane	Number of Images	GB-I (km)	GB-II (km)	Centroid (km)
Isabel 2003	21	105.75	87.31	174.74
Maria 2005	14	162.58	89.93	199.24

**Table 1:** Mean detected eye error for the GB method and the object centroid method.

### 5.2 Cyclone Tracking System Evaluation

We note that there is a correlation between the hurricane intensity and the tracking accuracy. Generally, more intense hurricanes are easier to detect using any of our cyclone eye detection algorithms as well-developed hurricanes have prominent features (well-formed vortex and log spiral shaped cloud bands). Hence, we use experimental results for the less intense hurricanes and not the stronger hurricanes (e.g. Category 5 Hurricane Katrina and Hurricane Rita in 2005) to show the robustness and strength of our system.

Method	Kalman Filter [4]	Particle Filter + Centroid	Particle Filter + GB-II
Error (km)	186.85	166.21	156.01

**Table 2:** Detected eye error for tracking Hurricane Maria using only the TRMM-adjusted precipitation images and QuikSCAT images.

We tracked Hurricane Maria for 5 days when the storm had already reached hurricane strength. Figure 3 shows one image for each of the three satellite image sources and the location of the automatically computed eye location from these images. (There were approximately 200 satellite images in the full track sequence). Figure 2 (Top) shows that the tracking result for Hurricane Maria by incorporating data from all three satellites is very close to the NHC best

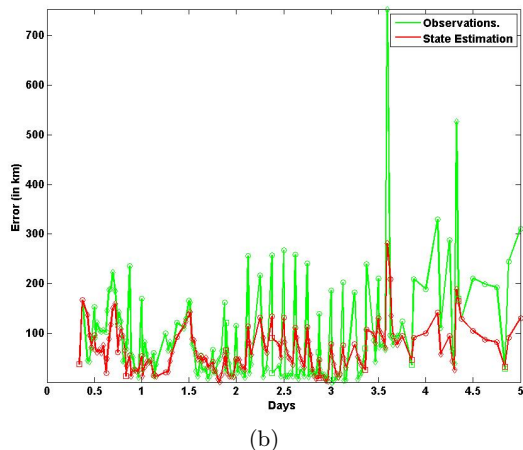
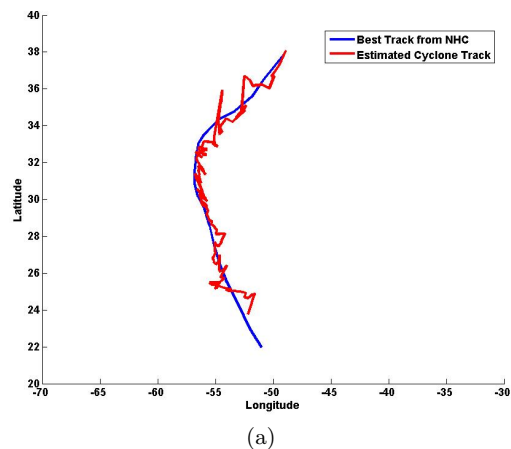


Figure 2: (a) Cyclone Track Comparison for Hurricane Maria. (b) Detected eye error comparison for state estimation and observations for Hurricane Maria. □: QuikSCAT observation, ○: TRMM observation, ◇: GOES observation.

track estimates. Figure 2 (Bottom) shows that the state estimation error is significantly smaller than the observation error for our tracker. The particle filter in this case effectively acts to smooth the observation errors. The mean state estimation error is 66.21km (see Table 3). It is clear from Table 2 and 3 that our system that includes GOES images performs much better than a system that does not include the GOES images for tracking Hurricane Maria.

Method	Kalman Filter [4] (km)	Particle Filter + Centroid (km)	Particle Filter + GB-II (km)
Maria	100.21	68.10	66.21
Ophelia	113.21	93.19	81.13
Philippe	265.36	203.40	193.42

Table 3: Detected eye error for cyclone tracking using the three satellite image sources.

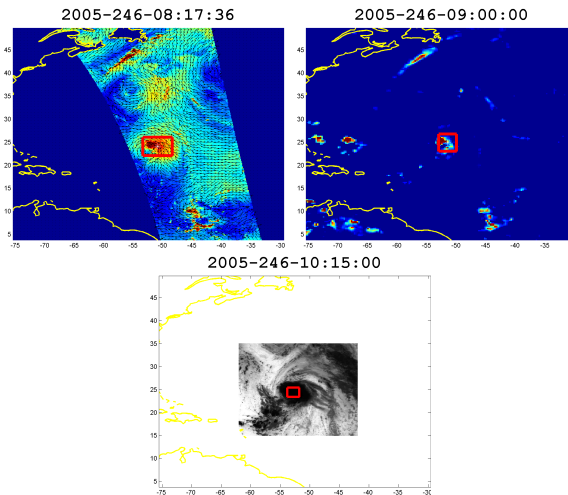


Figure 3: GOES, TRMM, QuikSCAT satellite images from Hurricane Maria. The detected eye is boxed in each image. The time at which each image was taken is also shown.

## Acknowledgments

This work was carried out at the Jet Propulsion Laboratory, California Institute of Technology with funding from the NASA Applied Information Systems Research (AISR) Program. The second author is supported by the NASA Postdoctoral Program (NPP) administered by Oak Ridge Associated Universities (ORAU) through a contract with NASA. ©2009 California Institute of Technology.

## 6. REFERENCES

- [1] R. Dunbar, T. Lungu, B. Weiss, B. Stiles, J. Huddleston, P. Callahan, G. Shirliffe, K. Perry, C. Hsu, C. Mears, F. Wentz, and D. Smith. *QuikSCAT Science Data Product User's Manual*. Jet Propulsion Laboratory, 2006.
- [2] V. F. Dvorak. *Tropical cyclone intensity analysis using satellite data*. NOAA Tech. Rep. NESDIS 11, 1984.
- [3] R. R. Halterman and D. G. Long. A comparison of hurricane eye determination using standard and ultra-high resolution quikscat winds. In *IEEE International Geoscience and Remote Sensing Symposium*, pages 4134–4137, 2006.
- [4] S.-S. Ho and A. Talukder. Automated cyclone discovery and tracking using knowledge sharing in multiple heterogeneous satellite data. In Y. Li, B. Liu, and S. Sarawagi, editors, *KDD*, pages 928–936. ACM, 2008.
- [5] S.-S. Ho and A. Talukder. Automated cyclone identification from remote quikscat satellite data. *IEEE Aerospace Conference*, 2008.
- [6] A. Wimmers and C. S. Welden. Satellite-based center-fixing of tropical cyclones: new automated approaches. In *Proceedings of the 26th Conference on Hurricanes and Tropical Meteorology*, 2004.
- [7] Q. P. Zhang, L. L. Lai, and H. Wei. Continuous space optimized artificial ant colony for real-time typhoon eye tracking. In *Proc. IEEE Int. Conf. on Systems, Man, and Cybernetics*, pages 1470–1475, 2007.